Effect of fiber length and surface treatment on the performance of fiber-modified binder

Preprint *in* Construction and Building Materials · March 2020

DOI: 10.1016/j.conbuildmat.2020.118702

7 authors, including:

Xiangyang Xing
Chang'an University
8 PUBLICATIONS **8** CITATIONS
SEE PROFILE

Liu Tao
□□□□
4 PUBLICATIONS **2** CITATIONS
SEE PROFILE

Rui Li
changan university
77 PUBLICATIONS **528** CITATIONS
SEE PROFILE

Jiupeng Zhang
Chang'an University
98 PUBLICATIONS **443** CITATIONS
SEE PROFILE

Construction and Building Materials 248 (2020) 118702

Contents lists available at ScienceDirect

Construction and Building Materials

journal homepage: www.elsevier.com/locate/conbuildmat

Effect of fiber length and surface treatment on the performance of fiber-modified binder

Xiangyang Xing [a], Tao Liu [a], Jianzhong Pei [a,*], Jianyou Huang [a], Rui Li [a], Jiupeng Zhang [a], Yefei Tian [b]

[a] School of Highway, Chang'an University, Xi'an 710064, China
[b] School of Materials Science & Engineering, Chang'an University, Xi'an 710064, China

HIGHLIGHTS

- Silane coupling agent improves the high temperature performance of aramid fiber modified asphalt.
- Silane coupling agent makes the surface of aramid fibers rough and hydrophobic.
- The increase of fiber length can improve the viscosity of fiber-modified asphalt binder.

ARTICLE INFO

Article history:
Received 3 June 2019
Received in revised form 24 February 2020
Accepted 8 March 2020

Keywords:
Aramid fibers
Asphalt binder
silane coupling agent KH-570
Surface treatment, rheological properties

ABSTRACT

In this study, the effects of fiber lengths and surface treatments of aramid fibers on the performance of aramid fiber-modified asphalt (AFMA) binders were examined. The surface treatment effects of aramid fibers with the silane coupling agent 3-methacryloxypropyltrimethoxysilane (KH-570) were investigated using scanning electron microscopy, a static contact angle method, and Fourier transform infrared spectroscopy. The length effects of the aramid fibers on the asphalt performance were studied using a dynamic shear rheometer, viscometer, and bending beam rheometer, and the improvement mechanisms were analyzed. The results show that an increase in fiber length can improve the viscosity of AFMA, and a reinforcement effect from short fibers with high content can be achieved by using long fibers with low content. It also indicated the silane coupling agent can enhance the bonding effect of fiber and asphalt. The results of this study can provide a reference for the application of fibers in asphalt binders and asphalt mixtures.

1. Introduction

Owing to increases in traffic volume and the number of heavy vehicles, as well as influences from environmental factors, asphalt pavement often suffers early damage far before the design life, seriously affecting the pavement performance [1–4]. As a high-strength, durable, and lightweight reinforcement material, fibers can significantly improve the mechanical properties of an asphalt mixture, improve the performance of asphalt pavement, and prolong the fatigue life of a pavement structure [5–11].

As compared with other organic fibers, aramid fibers are produced by polycondensation and spinning with an aromatic compound as a raw material, providing advantages in tensile strength and thermal stability, and showing better chemical resistance, a higher glass transition temperature, and a higher melting temperature [12–17]. Many scholars have studied the application of aramid fibers in asphalt mixtures. Klinsky et al. used polypropylene and aramid fibers in hot-mix asphalt, and found that the fibers improved the performance of the asphalt pavement, and reduced the occurrence of rutting, raveling, fatigue, and fracture [18]. Fazaeli et al. found that the simultaneous use of polyolefin-aramid fibers and sasobit in an asphalt mixture improved the durability and workability of the asphalt mixture [19]. Mirabdolazimi et al. determined that adding suitable polymer fibers to hot-mix asphalt improved the dynamic properties of an asphalt mixture [20]. Jaskuła et al. evaluated low-temperature cracking sensitivity using a constant deformation rate and rectangular beam bending test results from a semicircular bending test, based on a theory of fracture mechanics. The results showed that the use of aramid polyalphaolefin fibers improved the low-temperature performance of the pavement [21]. Hung et al. pointed out that aramid fibers generally exhibited better thermal stability and chemical resistance than conventional aliphatic fibers [22]. Badeli et al. found that aramid pulp fibers had a very high tensile strength and modulus,

* Corresponding author.
E-mail address: peijianzhong@126.com (J. Pei).

https://doi.org/10.1016/j.conbuildmat.2020.118702
0950-0618/

effectively improving the fatigue life of an asphalt mixture [12]. Eskandarsefat et al. showed that poly-functional fibers significantly improved the softening point and viscosity of asphalt, using conventional asphalt performance tests and a dynamic shear rheometer (DSR) [23]. Aliha used natural jute fibers and synthetic polyolefin-aramid fibers (FORTA) fibers to enhance warm-mix asphalt, and found that FORTA fibers provide better crack growth resistance than jute fibers [24]. Qian studied the effects of fiber pullout on the properties of an asphalt matrix composite using a fiber pullout test. As compared with polyester fibers, aramid fibers required a longer embedding length to fully activate their adhesion to asphalt [25]. In addition, some scholars have found that adding aramid fibers to a polymer composite can improve the glass transition temperature of the material, resulting in a high probability of thermal cracking [26–28].

However, the above studies have focused more on the influence of aramid fibers on the performance of an asphalt mixture; there is little research on the role of aramid fibers in an asphalt binder. Considering that the aramid fibers contact with the asphalt binder in an asphalt mixture first, the performance of aramid fiber-modified asphalt (AFMA) is very worthy of study, especially the impacts on the high- and low-temperature rheological performances of the asphalt binder. This paper introduces the results of such research.

In this study, the properties and modification mechanisms of AFMA with different fiber lengths were examined, and the technical feasibility of AFMA was discussed. As the surface of the aramid fibers is smooth and generally bundle-shaped, the fibers are not easy to disperse. To enhance the adhesion of the aramid fibers and asphalt, the surface of the aramid fibers was treated with the silane coupling agent 3-methacryloxypropyltrimethoxysilane (KH-570). The static contact angle, surface grafting effect, and microscopic morphology of the aramid fibers were tested before and after the surface treatment. The high-temperature rheological properties of AFMA were analyzed using a DSR and viscometer. The low-temperature performance of AFMA was studied using a bending beam rheometer (BBR). In general, the rheological properties of AFMA with different lengths of aramid fibers were studied, from micro to macro.

2. Material and methods

2.1. Raw material

2.1.1. Base asphalt

In this study, PG58-28 was selected as the base asphalt. The tests were carried out according to Chinese Standards (JTG E20-2011) [29]. The performance properties are shown in Table 1.

2.1.2. Aramid fibers

The different lengths of the aramid fibers were produced by the Tellus New Material Corporation, Shenzhen. The appearance of the aramid fibers was golden yellow. In this study, to study the effect of fiber length on the asphalt binder, four different lengths of aramid fibers (1 mm, 2 mm, 3 mm, and 6 mm) were selected, as shown in Fig. 1.

The characteristics of the aramid fibers are shown in Table 2.

Table 1
Properties of base asphalt.

Test items	Measured values	Standard
Density (15 °C), g/cm,	1.003	T0603-2011
Viscosity (135 °C), Pa·s	0.374	T0625-2011
Penetration (25 °C), 0.1 mm	88.9	T0604-2011
Ductility (15 °C, 5 cm/min), cm	>100	T0605-2011
Softening Point (Ring-and-Ball), °C	45.1	T0606-2011

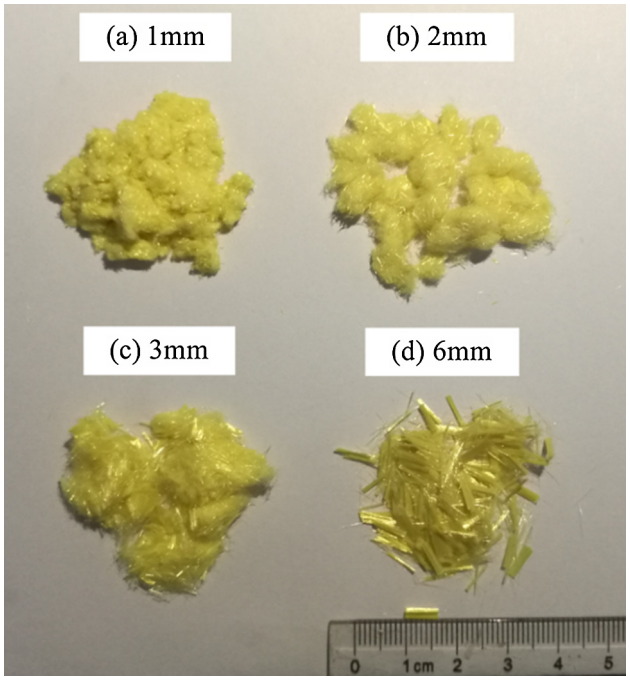

Fig. 1. Aramid fibers' appearance (1 mm, 2 mm, 3 mm, and 6 mm).

2.1.3. Silane coupling agent and other chemical reagents

The silane coupling agent KH-570 is a widely used coupling agent, and is not only soluble in water but is also soluble in organic solvents such as ethanol and toluene. The anhydrous ethanol used in this study was produced by the Beijing Chemical Reagent Company. The water used in this study was distilled water.

2.2. Preparation of aramid fiber-modified asphalt (AFMA)

2.2.1. Aramid fibers surface treatment

Owing to the steric effect of the aramid fiber benzene ring and the high crystallinity of the molecular chain, untreated aramid fibers have a smooth surface, low chemical activity, and a weak interfacial adhesion to base asphalt, resulting in poor performance in an asphalt binder [30].

(1) Anhydrous ethanol and distilled water were prepared in ethanol solution at a ratio of 3:7. Then, KH-570 was added into the above ethanol solution, by 2 wt% of the ethanol solution. The mixture was thoroughly stirred and allowed to stand for 30 min, to sufficiently hydrolyze the silane coupling agent.
(2) The aramid fibers were added to the solution of step (1), and immersed for 60 min.
(3) The aramid fibers were recovered and placed in an oven at 80 °C for 3 h for drying [31]. Accordingly, surface-treated aramid fibers were obtained. The surface treatment process of the aramid fibers is shown in Fig. 2.

2.2.2. Preparation of AFMA

When manufacturing fiber asphalt using a high-speed shearing method, the integrity of fibers can be destroyed, and the modification effect on asphalt can be affected. In this study, a low-speed agitation method was used. The preparation process of the AFMA is as follows:

Table 2
Characteristics of aramid fibers.

Diameter(μm)	Specific Gravity(g/cm^3)	Decomposition Temperature(°C)	Elongationat Break(%)	TensileStrength(GPa)
12	1.44	430–550	3.6	2.76

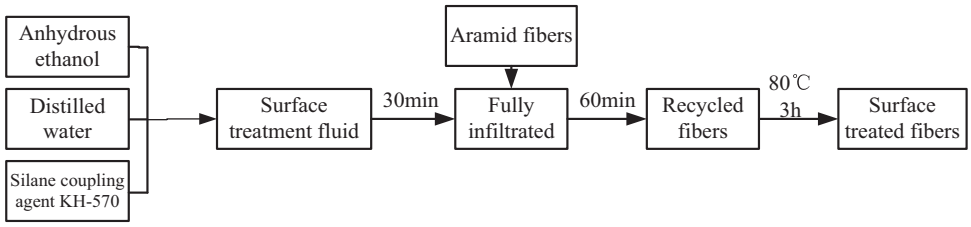

Fig. 2. Aramid fibers' surface treatment process.

(1) The aramid fibers were weighed by 2 wt% of the asphalt.
(2) The asphalt was placed in an oven and heated to 150 °C. Then, 300 g of asphalt was weighed in a stainless steel beaker, and the beaker was placed in a constant temperature oil bath at 150 °C.
(3) The electric mixer was turned on. The above-mentioned weighed aramid fibers were gradually added to the asphalt in several iterations, and stirring was continued for 30 min until the aramid fibers were uniformly dispersed.

The preparation process of the AFMA is shown in Fig. 3.

2.3. Test methods

2.3.1. Scanning electron microscope (SEM)

The morphology and phase composition of the aramid fibers are important indicators for evaluating the properties of the fibers. In this study, a scanning electron microscope (SEM) was used to detect the microstructure of the aramid fibers before and after the surface treatment.

In the test, a conductive double-sided adhesive was pasted on a sample disk, and then the aramid fiber was carefully pasted on the double-sided adhesive; the unstuck fiber was blown off using an ear ball. During the test, sterile gloves were worn, and the sample was clamped with tweezers. Finally, the samples were sprayed with gold, and then scanned by the SEM. The test voltage was 5 kV, and the magnification was conducted 150, 200, and 2000 times.

2.3.2. Water contact angle

The contact angle of aramid fibers to a liquid can indirectly reflect a treatment effect on the fibers' surface. In this study, a sessile drop method [32,33] was used to measure the contact angle between the aramid fibers and water. The volume of the droplets was 6 μL, and the titration speed was 80 μL/min. The equipment could realize fully automatic operation, and after the liquid titration, it automatically measured the water contact angle. The selected measurement contact time was 60 s.

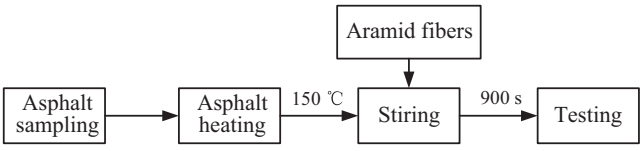

Fig. 3. Preparation process of aramid fiber-modified asphalt (AFMA).

2.3.3. Fourier transform infrared spectroscopy (FT-IR)

The effects of the aramid fibers before and after surface treatment were detected using Fourier transform infrared spectroscopy (FT-IR). The wave number range of the test was 4000–500 cm^{-1}. In this study, 2–3 mg of 1 mm aramid fibers were mixed with dry KBr powder via tablet pressing. The mixture was ground into a fine powder in a mortar, and then was placed into a mold to make a test sample piece for rapid testing, to prevent the moisture absorption of the sample piece from affecting the accuracy of the results.

2.3.4. Dynamic shear rheometer test (DSR)

The various AFMA samples were tested in accordance with a specification (American Association of State Highway and Transportation Officials (AASHTO) T 315-12 and TP 70-11). The National Cooperative Highway Research Program 9-10 project proposed using a repeated creep recovery (RCR) test to evaluate the high-temperature rutting resistance of an asphalt binder. D'Angelo et al. subsequently proposed a relatively simple and fast multiple stress creep recovery (MSCR) test evaluation index based on the RCR test. The MSCR test can better reflect the nonlinear viscoelastic response of modified asphalt, and J_{nr} has been proven to have a good correlation with the rutting performance of modified asphalt [34,35]. The method used two stress levels (0.1 kPa and 3.2 kPa) for continuous testing. Each stress level was 10 cycles, and each cycle was 10 s, including a 1 s creep phase and a 9 s unload recovery phase. The total test time was 200 s. To improve the accuracy, two repetitions were considered for each type of sample. The final evaluation index comprises the deformation recovery rate (R) and irreversible compliance (J_{nr}). The R and J_{nr} values in each loading cycle were calculated as follows:

$$R = (\gamma_P - \gamma_{nr})/\left(\gamma_p - \gamma_0\right) \tag{2-1}$$

$$J_{nr} = (\gamma_{nr} - \gamma_0)/\tau \tag{2-2}$$

Here, γ_p is the peak strain in each loading cycle, γ_{nr} is the residual strain in each loading cycle, and γ_0 is the initial strain in each loading cycle.

2.3.5. Rotational viscosity (RV) test

The viscosity of asphalt can reflect the ability of an asphalt binder to resist shear deformation under external forces. The test was conducted in accordance with an AASHTO specification (AASHTO T 316-13). Before the test, the prepared AFMA was placed into a sample container, kept in an oven at 150 ℃ for 30 min, and then poured into the sample container of the viscometer. The viscosity of the AFMA at a constant temperature of 135 °C was measured at the speed of 20 rpm with the 27# spindle.

2.3.6. Bending beam rheometer test (BBR)

The United States Strategic Highway Research Program (SHRP) proposed using the BBR test to evaluate the low-temperature performance of an asphalt binder. In this study, and in accordance with the standard method of the BBR test (AASHTO T 313-09) [36], the AFMA was processed into samples (6.4 ± 0.1 mm thick by 12.7 ± 0.25 mm wide by 127 ± 5 mm long) using a special mold. The BBR test is a loading test conducted using the equipment's own software. The specimen was loaded at a constant stress for 240 s at −6 °C, −12 °C, and −18 °C, respectively. The stiffness modulus (S) and creep rate (m) at 60 s were used to evaluate the low-temperature performance of the AFMA specimens.

3. Results and discussion

3.1. Effect of surface treatment for the bonding properties of aramid fibers and asphalt

3.1.1. SEM microphotos of aramid fibers

Fig. 4(a) and (b) show the SEM results before surface treatment of the aramid fibers, and (c) and (d) show the SEM results after the surface treatment. As can be seen from the figures, the diameter of the aramid fiber is approximately 12 μm. The original aramid fibers are arranged in a bundle with a smooth surface, i.e., they are closely arranged and not easy to disperse. After treatment with KH-570, the surface of the aramid fibers is coated with a layer of reagent, and the surface becomes rough. It can be further determined that the reagent layer on the surface of an aramid fiber does not completely cover the fiber itself. Some of the darker parts may be uncoated, or the reagent layer peeled off. The silane coupling agent reagent layer on the fiber surface can facilitate the fiber and asphalt becoming more tightly combined, but also makes the aramid fibers less likely to agglomerate, improving the dispersibility of the chopped aramid fibers.

3.1.2. Water contact angle

In this study, the droplet volume was 6 μL, and the titration rate was 80 μL / min. If the droplets are too large, they will not remain spherical, which can easily cause measurement errors. The static contact angle has a time effect, that is, the contact angle is different when measured at different contact times. For water droplets, the contact time is generally selected as 60 s. Fig. 5 shows the water contact angle of the aramid fibers before and after surface treatment with the silane coupling agent KH-570. Generally, the size of the water contact angle is a criterion for determining wettability. If the water contact angle = 0, the water wets the solid surface, and spreads over it. If the water contact angle = 180°, there is no wetting at all, and the water condenses into small spheres on the solid surface. It can be observed from Fig. 5 that the water contact angle is close to zero before treatment, and that the water substantially completely wets the surface of the aramid fibers. After treatment, the water contact angle measurements were 130.3° and 131.7°.

The change of the water contact angle indicated that the wettability of the aramid fibers changed significantly after KH-570 treatment. According to the Cassie-Baxter model theory, the wettability of a solid surface is determined by its surface energy and microstructure. The smaller the solid surface energy, the larger the contact angle of the liquid on the solid surface, and the less likely the solid is to be wetted by the liquid [37,38]. As shown in the SEM scanning results, the KH-570 forms a coating on the surface of the aramid fibers, which not only makes the surface of aramid fibers rough, but also reduces their surface energy. In such a case, an aramid fiber is more difficult to wet (by water); this is beneficial for preventing water damage when the fiber is used in asphalt pavement.

3.1.3. Ft-ir

Fig. 6 is the FT-IR result for the aramid fibers, before and after surface treatment with KH-570. It shows that the stretching

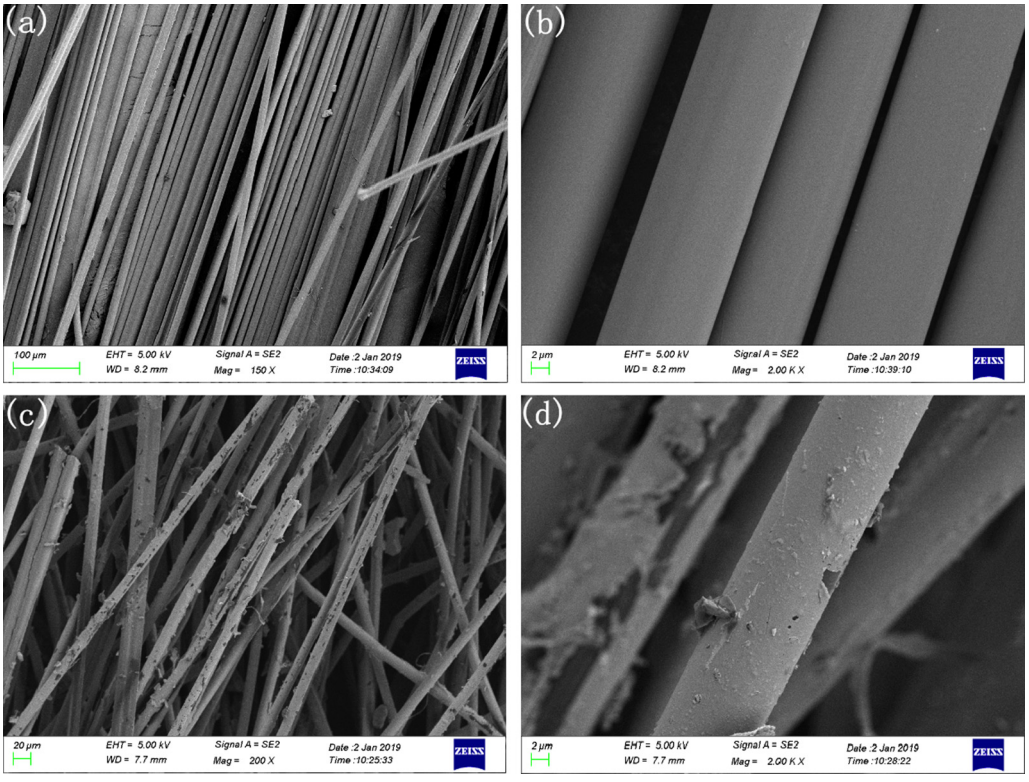

Fig. 4. Microphotos before and after surface treatment of aramid fibers (a) 150 times (b) 2000 times, before treatment; (c) 200 times (d) 2000 times, after treatment.

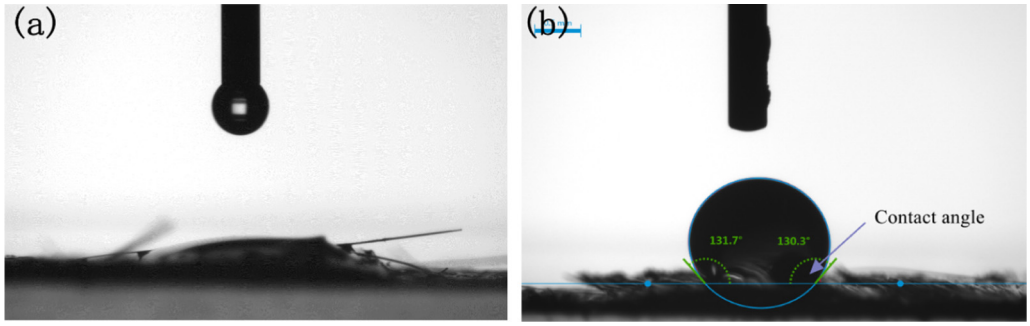

Fig. 5. Water contact angle of aramid fibers before and after surface treatment (a) before treatment; (b) after treatment.

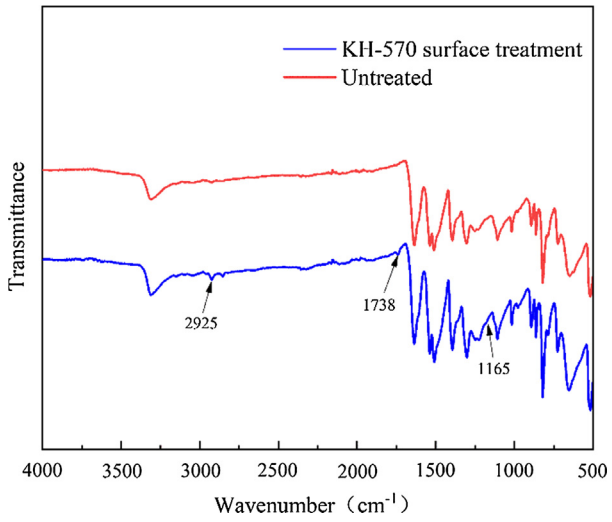

Fig. 6. Fourier transform infrared spectroscopy (FT-IR) results of aramid fibers before and after surface treatment.

vibration peak of C–H appears at 2925 cm^{-1}, which is the methyl peak; the stretching vibration peak of the carbonyl group appears at 1738 cm^{-1}; and the Si-O stretching vibration peak appears at 1165 cm^{-1}. The above characteristic peaks are the characteristic peaks of KH-570. The results indicate that the KH-570 has been successfully grafted onto the surface of aramid fibers and has attracted double bonds.

The coupling agent has a bifunctional group in the chemical structure, and acts as a "bridge" in the composite material. One end reacts with the surface of the fibers, and the other end reacts with the base asphalt to form a coupling agent bridging and entanglement between the fibers and the base asphalt [31]. Thereby, the improved interfacial transition zone improves the interface structure, and eliminates the sudden change in stress, significantly improving the transverse tensile strength of the composite material. After hydrolysis of KH-570, the $-(OCH_3)_3$ group is hydrolyzed to form –OH, which reacts with the –OH of asphalt, whereas the organic functional group at the other end reacts with the –COOH group of aramid fibers, which can form an organic bond between aramid fibers and asphalt, thereby improving the bonding degree between the fibers and asphalt.

3.2. High temperature rheological properties of AFMA

3.2.1. Temperature creep test

It can be seen from Fig. 7(a) that the respective complex shear moduli (G*) of the various types of AFMA are higher than that of the base asphalt. As the temperature increases, the G* of the various types of AFMA show a downward trend. In the high-temperature range of 50 to 80 °C, as the length of the aramid fibers increases, the G* gradually increases. The AFMA with surface-treated aramid fibers have higher G* than untreated AFMA, indicating that the aramid fibers are more tightly bonded to the asphalt. In that regard, AFMA is as temperature sensitive as the base asphalt.

As shown in Fig. 7(b), from 50 to 80 °C, the respective phase angle of the various types of AFMA increases with increasing temperature. As the lengths of the aramid fibers increase, the phase angle gradually decreases, indicating that elastic characteristics of the asphalt binders have been enhanced. For AFMA with 3 mm-aramid fibers, when the temperature reaches 70 °C or above, the phase angle curves gradually become flat. This indicates that at high temperature, 3 mm-aramid fiber shows a more stable effect on the rheological properties of asphalt. The surface-treated AFMA has a smaller phase angle than untreated AFMA, indicating that after the surface treatment, the fibers and asphalt are more tightly combined.

The rutting factor ($G^*/\sin\delta$) is a comprehensive manifestation of the viscoelastic properties of an asphalt binder and is an important indicator for evaluating the high-temperature rheological properties of asphalt and the anti-rutting performances of asphalt mixtures. The rutting factor variations of various asphalt binders with temperature are shown in Fig. 8. It can be seen that the change trends of $G^*/\sin\delta$ with temperature are basically similar to that of $G^*/\sin\delta$ of AFMA but different in size, but the variations with the test temperature are consistent. Temperature is a key factor affecting the high-temperature rheological properties of AFMA. After fibers are added, the $G^*/\sin\delta$ of AFMA is slightly improved as compared with base asphalt. The addition of fibers improves the high-temperature rutting resistance of asphalt. The main reason is that the aramid fibers were dispersed in the asphalt, and the massive surface area became the contact interface layer. In the interface layer, a part of asphalt binder adhered to the surface of the fibers to form a structural asphalt layer, which was more adhesive than the free asphalt out over the interface layer, thereby improving the bonding performance of the asphalt. Meanwhile, the aramid fibers formed a three-dimensional network structure in the asphalt, improving the shear deformation resistance of the asphalt. However, with the increase in temperature, the stability of the fibers in the asphalt was weakened, the free asphalt in the AFMA gradually increased, and the $G^*/\sin\delta$ of the AFMA with different lengths gradually approached zero.

3.2.2. Multiple stress creep recovery (MSCR)

To evaluate and compare the stress recovery properties of AFMA with different fiber lengths, the experimental temperature selected in this study was 64 °C. This was mainly because rutting on asphalt pavements is more likely to occur above 60 °C. The trend of data changes during the experiment is shown in Fig. 9.

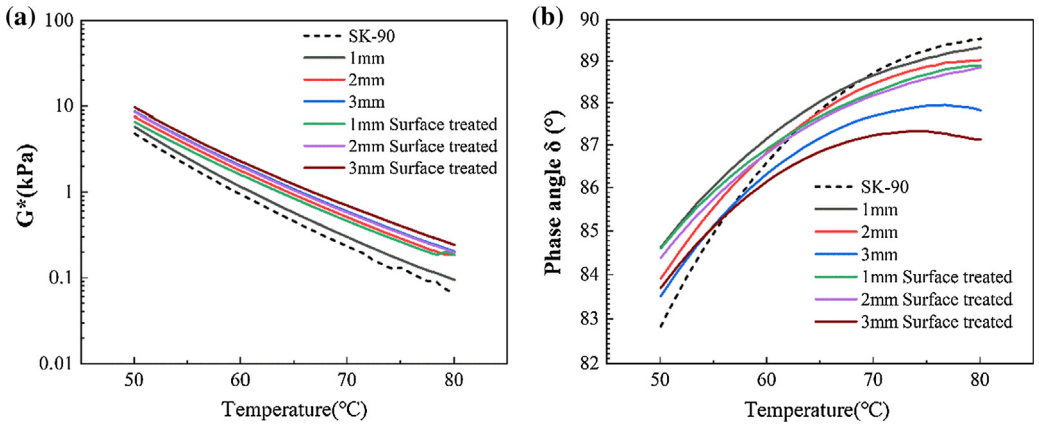

Fig. 7. Complex shear modulus and phase angle results.

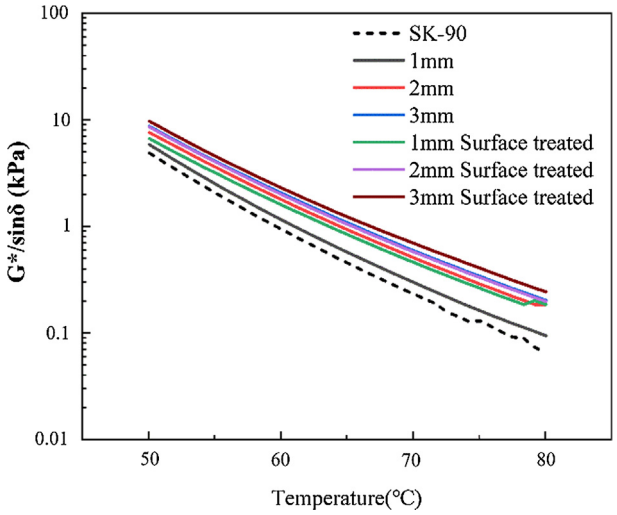

Fig. 8. Rutting factor variations of various asphalt binders.

According to Eqs. (2-1) and (2-2), Table 3 shows the results for the average strain recovery rate (R) and average unrecoverable creep compliance (J_{nr}).

It can be seen from Table 3 that with the increase in the length of the aramid fibers, the R values of asphalt gradually increase, and the J_{nr} values gradually decrease at 0.1 kPa. The results show that under light-load traffic pressure, with an increase in the length of the aramid fibers, the deformation recovery ability of the AFMA increases gradually, improving the elasticity and anti-rutting ability of the asphalt binder. As compared with 0.1 kPa, the R values increase slowly, and the J_{nr} values continue to increase at 3.2 kPa. This shows that under heavy traffic, the elastic recovery increases slowly, and permanent deformation is more likely to occur.

3.2.3. Viscosity

Fig. 10 depicts samples of AFMA with different lengths of aramid fibers, at the same content (2 wt% of asphalt binder). As can be seen from the figure, the viscosities of the AFMA samples with the same weight are significantly different, and thus the flow expansion areas are also different. As compared to AFMA with 1 mm and 2 mm aramid fibers, the 3 mm-AFMA has become very viscous, whereas the 6 mm-AFMA has completely become a viscous paste. The reason is that with the increase in aramid fibers' length, a three-dimensional fiber network is gradually formed in asphalt binder. Moreover, the interlacing and winding effects between fibers becomes more evident, making the AFMA become more viscous.

As shown in Fig. 11, as the fiber content increases, the viscosity of AFMA with different lengths of aramid fibers gradually increases. The viscosity growth of AFMA with 1 mm or 2 mm aramid fibers is basically stable. When the fiber content is 1%, the viscosity values of the two AFMA samples are close, and slightly higher than that of base asphalt (0.374 Pa·s), indicating that the

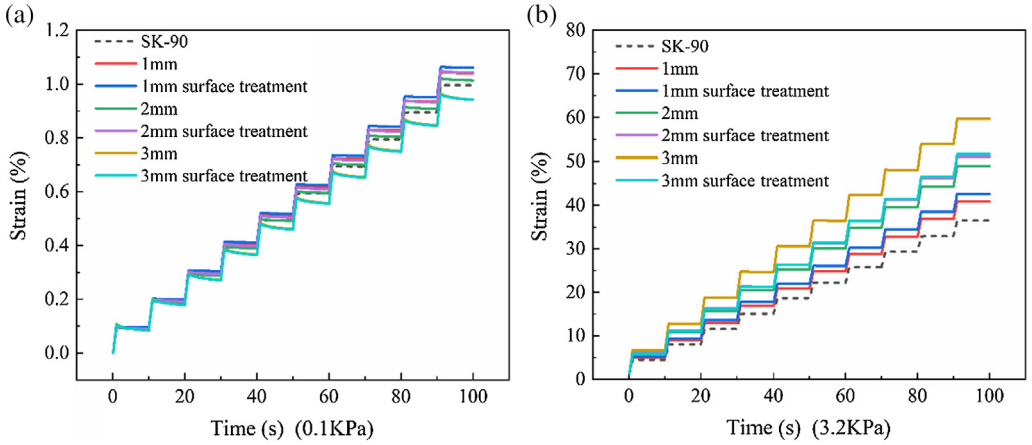

Fig. 9. Multiple stress creep recovery (MSCR) curves of various AFMA and base asphalt.

Table 3
Calculation results for R and J_{nr}.

Asphalt binder	0.1 kPa				3.2 kPa			
	R (%)	Error (%)	J_{nr} (kPa^{-1})	Error (%)	R (%)	Error (%)	J_{nr} (kPa^{-1})	Error (%)
Base asphalt binder	0.93	4.3	0.93	12.3	0.02	5.2	1.03	10.7
Aramid fiber-modified asphalt (AFMA) (1 mm)	2.43	3.9	0.97	11.9	0.06	4.3	1.15	8.9
(1 mm Surface treatment)	3.21	4.3	0.98	7.8	0.12	6.1	1.21	7.3
(2 mm)	7.46	4.5	0.93	10.6	0.37	5.7	1.39	14.8
(2 mm Surface treatment)	7.91	5.2	0.96	6.9	0.28	7.3	1.45	11.2
(3 mm)	20.24	6.1	0.84	12.3	0.79	6.4	1.46	13.7
(3 mm Surface treatment)	21.80	4.9	0.83	12.7	0.80	5.2	1.71	9.8

Fig. 10. Samples of AFMA with different lengths.

fibers act as particle-like filler into the asphalt matrix. The viscosity of the asphalt binder with 3 mm aramid fibers has a large jump from 1% to 2%, indicating that the fiber network reinforcing effect becomes remarkable. When the fiber content is 4%, the 3 mm-aramid fibers have become a non-uniform viscous solid, so the viscosity cannot be measured. Under a condition of constant fiber content, with the increase in fiber length, the viscosity of AFMA increases gradually. A reinforcement effect from short fibers with high content can be achieved by using long fibers with low content. For example, when the viscosity is 2500 mPa·s, the contents of the 1 mm, 2 mm, and 3 mm-aramid fibers are 3.6%, 2.3%, and 1.3%, respectively.

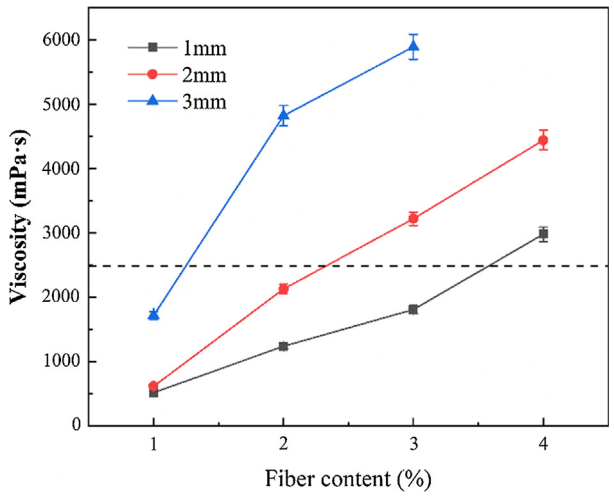

Fig. 11. The viscosity of AFMA at 135 °C.

3.3. Low-temperature rheological properties of AFMA

Thermoelectric BBR equipment was used to test the stiffness modulus (S) and creep rate (m) values of AFMA at −6 °C, −12 °C, and −18 °C. Fig. 12 shows the effects of fiber length and surface treatment on the stiffness and creep rate m-values of AFMA.

According to the BBR test method, S represents the stiffness modulus of the asphalt, and the m- value represents the rate at which the asphalt releases contraction stress through its own viscoelastic flow [36]. The stress generated by the increase in the stiffness of low-temperature asphalt can be released by its own viscoelastic flow. The low stiffness and high release rate are beneficial to asphalt against low-temperature cracking. Therefore, to reduce the cracking of road surfaces, the SHRP performance specification limits the S and m-values at 60 s to be not more than 300 MPa and 0.3, respectively.

Fig. 12(a) shows the stiffness curves of various types of AFMA at different temperatures (−6, −12, and −18 °C). It can be seen that with the increase in temperature from −18 °C to −6 °C, the stiffness values of various types of asphalt binders show a downward trend. Under the same test temperature conditions, the stiffness of the asphalt binders gradually increases with the increases in the length of the aramid fibers. AFMA with surface-treated aramid fibers has a lower stiffness than untreated AFMA, as treated aramid fibers have a rougher surface and may be more closely integrated with the asphalt binder. In general, the stiffness of the base asphalt binder is slightly smaller than in the other various types of AFMA.

The m-value characterizes the relaxation ability of the asphalt. The larger the m-value, the stronger the relaxation ability. When the temperature drops sharply, such materials tend to have better low-temperature performance. Fig. 12(b) shows the trends of m-value changes for various types of asphalt at different temperatures. From −18 °C to −6 °C, with the increase in temperature, the m values of the various types of asphalt show an increasing trend. It can be seen that under the same temperature conditions, the m-value gradually decreases as the fiber length increases. The m-values of the various types of AFMA are less than 0.3, which does not meet the requirements of the "Superpave" specification. This indicates that the addition of aramid fibers to asphalt has a negative effect on the low-temperature performance of asphalt. Some scholars have found that adding aramid fibers to polymer composites can improve the glass transition temperature of materials, resulting in a high probability of thermal cracking.

From the above results regarding the low-temperature rheological properties of AFMA, it can be found that the stiffness values of AFMA are higher than those of base asphalt at the same temperature, and that the m-values are smaller than those of base asphalt. The low-temperature performance of AFMA is not as good as that of base asphalt. The above results are analyzed as follows. The aramid fibers effectively increase the viscosity of the asphalt, resulting in an increase in the stiffness modulus of the asphalt and a decrease in flexibility. The chopped aramid fibers are more similar

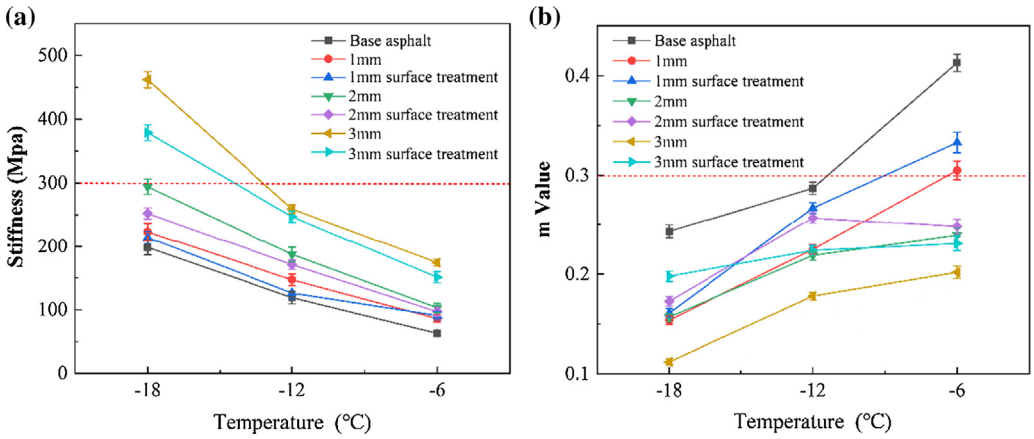

Fig. 12. Stiffness and m-value curves of various types of asphalt binder (a) Stiffness curves; (b) m-value curves.

to particle-reinforcing material, which can improve the high-temperature deformation resistance of asphalt. However, the low-temperature crack resistance and toughening effects are not good. The addition of aramid fiber can also increase the glass transition temperature of AFMA and cause a decrease in its low-temperature performance. However, the BBR test only evaluates the low-temperature performance of asphalt from the aspects of creep stiffness and creep rate, and cannot fully reflect the elongation performances of AFMA. Therefore, it is difficult to evaluate the toughening effects of fibers in the asphalt.

4. Conclusions

In this study, a surface treatment effect on aramid fibers was characterized using a SEM, contact angle, and FT-IT. Then, the length effect of the aramid fibers on AFMA was studied via DSR, RV, and BBR tests. From the above study, the following conclusions can be drawn:

(1) The use of aramid fibers to reinforce asphalt can improve the high-temperature performance of the asphalt. However, the dispersion of fibers is very important for fiber-modified asphalt. Fibers with a length of 6 mm are easily agglomerated, so that they are not uniformly dispersed in the asphalt binder.
(2) In terms of the viscosity index, the viscosity of AFMA will rise with the increase in fiber content; under the same content, the viscosity of AFMA will also increase with the use of longer fibers, which can reflect the evident fiber length effect. An increase in fiber content or fiber length can improve the viscosity of fiber-modified asphalt.
(3) The results from the SEM, contact angle, and FT-IR tests show that silane coupling agent successfully adheres to the surface of the aramid fibers, forming a film that does not completely cover the surface of fibers, making the surface of aramid fibers rough and hydrophobic.
(4) Further discussion is required on whether the BBR test can evaluate the low-temperature properties of AFMA well. A thermal stress-restricted specification test (TSRST) can directly obtain the curves of cracking and temperature stress at low temperature, and is an effective method for studying the low-temperature cracking resistance of an asphalt mixture. In the future, TSRST can be used to study the low-temperature crack resistance of the fiber-asphalt mixture.

CRediT authorship contribution statement

Xiangyang Xing: Conceptualization, Data curation, Writing - original draft. **Tao Liu:** Visualization, Investigation, Formal analysis. **Jianzhong Pei:** Supervision. **: . Jianyou Huang:** Software, Validation. **Rui Li:** Methodology. **Jiupeng Zhang:** Writing - review & editing. **Yefei Tian:** Visualization.

Declaration of Competing Interest

The authors declare that they have no known competing financial interests or personal relationships that could have appeared to influence the work reported in this paper.

Acknowledgements

This study was supported by National Key R&D Program of China (Grant No. 2018YFE0103800), National Key Research and Development Program of the Ministry of Science & Technology of China (Nos. SQ2018YFGH000187), the Department of Science & Technology of Shaanxi Province (Nos. 2016ZDJC-24, and 2017KCT-13), the Special Fund for Basic Scientific Research of Central College of Chang'an University (Nos. 300102219316). The authors gratefully acknowledge their financial support.

References

[1] G.D. Airey, A.C. Collop, S.E. Zoorob, R.C. Elliott, The influence of aggregate, filler and bitumen on asphalt mixture moisture damage, Constr. Build. Mater. 22 (9) (2008) 2015–2024.
[2] C. Gorkem, B. Sengoz, Predicting stripping and moisture induced damage of asphalt concrete prepared with polymer modified bitumen and hydrated lime, Constr. Build. Mater. 23 (6) (2009) 2227–2236.
[3] S. Tayfur, H. Ozen, A. Aksoy, Investigation of rutting performance of asphalt mixtures containing polymer modifiers, Constr. Build. Mater. 21 (2) (2007) 328–337.
[4] G. Liu, Y. Tao, L. Jing, Y. Jia, Y. Zhao, J. Zhang, Effects of aging on rheological properties of asphalt materials and asphalt-filler interaction ability, Constr. Build. Mater. 168 (2018) 501–511.
[5] S.M. Abtahi, M. Sheikhzadeh, S.M. Hejazi, Fiber-reinforced asphalt-concrete – A review, Constr. Build. Mater. 24 (6) (2010) 871–877.
[6] H. Chen, Q. Xu, S. Chen, Z. Zhang, Evaluation and design of fiber-reinforced asphalt mixtures, Mater. Des. 30 (7) (2009) 2595–2603.
[7] J. Zhang, Z. Fan, H. Wang, W. Sun, J. Pei, D. Wang, Prediction of dynamic modulus of asphalt mixture using micromechanical method with radial distribution functions, Mater. Struct. 52 (2) (2019) 49–58.
[8] A. Norhidayah, Y. Haryati, M. Nordiana, M.M.K. Idham, A. Juraidah, P. Ramadhansyah, Permeability coefficient of porous asphalt mixture containing coconut shells and fibres, IOP Conference Series: Earth and Environmental Science, IOP Publishing, 2019.

[9] Y. Haryati, A. Norhidayah, M. Nordiana, A. Juraidah, A.N. Hayati, P. Ramadhansyah, M.K. Azman, A. Haryati, Stability and rutting resistance of porous asphalt mixture incorporating coconut shells and fibres, IOP Conference Series: Earth and Environmental Science, IOP Publishing, 2019.
[10] T. Ting, P. Ramadhansyah, A. Norhidayah, H. Yaacob, M. Hainin, M.W. Ibrahim, D. Jayanti, A. Abdullahi, in: Effect of Treated Coconut Shell and Fiber on the Resilient Modulus of Double-layer Porous Asphalt, Science, IOP Publishing, 2018, p. 012065.
[11] M. Hainin, M. Idham, N. Yaro, S. Hussein, M. Warid, A. Mohamed, S. Naqibah, P. Ramadhansyah, Performance of Hot Mix Asphalt Mixture Incorporating Kenaf Fibre, IOP Conference Series: Earth and Environmental Science, IOP Publishing (2018) 012092.
[12] S. Badeli, A. Carter, G. Doré, S. Saliani, Evaluation of the durability and the performance of an asphalt mix involving Aramid Pulp Fiber (APF): complex modulus before and after freeze-thaw cycles, fatigue, and TSRST tests, Constr. Build. Mater. 174 (C) (2018) 60–71.
[13] M.-J. Kim, S. Kim, D.-Y. Yoo, H.-O. Shin, Enhancing mechanical properties of asphalt concrete using synthetic fibers, Constr Build Mater 178 (2018) 233–243.
[14] H.M. Yang, Aramid Fibers, in: P.W.R. Beaumont, C.H. Zweben (Eds.), Comprehensive Composite Materials II, Elsevier, Oxford, 2018, pp. 187–217.
[15] X.Y. Xing, J.Z. Pei, R. Li, X.Y. Tan, Effect and mechanism of calcium carbonate whisker on asphalt binder, Mater. Res. Express 6 (5) (2019).
[16] X. Tan, J. Zhang, D. Guo, G. Sun, B. Zhou, W. Zhang, Preparation and Repeated Repairability Evaluation of Sunflower Oil-Type Microencapsulated Filling Materials, J. Nanosci. Nanotechnol. 20 (3) (2020) 1554–1566.
[17] J.P. Zhang, X.Q. Li, W.S. Ma, J.H. Pei, Characterizing Heterogeneity of Asphalt Mixture Based on Aggregate Particles Movements, Iranian Journal of Science & Technology Transactions of Civil Engineering 43 (1) (2018) 1–11.
[18] L.M.G. Klinsky, K.E. Kaloush, V.C. Faria, V.S.S. Bardini, Performance characteristics of fiber modified hot mix asphalt, (2018).
[19] H. Fazaeli, Y. Samin, A. Pirnoun, A.S. Dabiri, Laboratory and field evaluation of the warm fiber reinforced high performance asphalt mixtures (case study Karaj – Chaloos Road), Constr. Build. Mater. 122 (2016) 273–283.
[20] S.M. Mirabdolazimi, G. Shafabakhsh, Rutting depth prediction of hot mix asphalts modified with forta fiber using artificial neural networks and genetic programming technique, Constr. Build. Mater. 148 (2017) 666–674.
[21] P. Jaskuła, M. Stienss, C. Szydłowski, Effect of Polymer Fibres Reinforcement on Selected Properties of Asphalt Mixtures ☆, Procedia Eng. 172 (2017) 441–448.
[22] C.H.Z. Hung Man Yang, Peter W.R. Beaumont, Aramid Fibers,, Comprehensive Composite Materials II, (2018) 187-217.
[23] S. Eskandarsefat, B. Hofko, C.O. Rossi, C. Sangiorgi, Fundamental properties of bitumen binders containing novel cellulose-based poly-functional fibres, Compos. B Eng. 163 (2019) 339–350.
[24] M.R.M. Aliha, A. Razmi, M. Razavi, A. Mansourian, The influence of natural and synthetic fibers on low temperature mixed mode I+II fracture behavior of warm mix asphalt (WMA) materials, Eng. Fract. Mech. 182 (2017). S0013794417303843.
[25] S. Qian, M. Hui, J. Feng, R. Yang, X. Huang, Fiber reinforcing effect on asphalt binder under low temperature, Constr. Build. Mater. 61 (7) (2014) 120–124.
[26] Y. Sun, Y. Zhang, K. Xu, W. Xu, D. Yu, L. Zhu, H. Xie, R. Cheng, Thermal, mechanical properties, and low-temperature performance of fibrous nanoclay-reinforced epoxy asphalt composites and their concretes, J Appl Polym Sci 132 (12) (2015).
[27] W. Lertwassana, T. Parnklang, P. Mora, C. Jubsilp, S. Rimdusit, High performance aramid pulp/carbon fiber-reinforced polybenzoxazine composites as friction materials, Compos. B Eng. 177 (2019) 107280.
[28] M. Wirti, G.R.R. Biondo, D. Romanzini, S.C. Amico, A.J. Zattera, The effect of fluorination of aramid fibers on vinyl ester composites, Polym. Compos. 40 (5) (2019) 2095–2102.
[29] M.o.T.o.t.P.s.R.o. China, Standard Test Methods of Bitumen and Bituminous Mixtures for Highway Engineering, (JTG E20-2011) (2011).
[30] C. Jia, P. Chen, W. Liu, B. Li, Q. Wang, Surface treatment of aramid fiber by air dielectric barrier discharge plasma at atmospheric pressure, Appl. Surf. Sci. 257 (9) (2011) 4165–4170.
[31] X. Yu, X. Youjun, L. Guangcheng, Effect of basalt fiber surface silane coupling agent coating on fiber-reinforced asphalt: From macro-mechanical performance to micro-interfacial mechanism, Constr. Build. Mater. 179 (2018) 107–116.
[32] J. Drelich, Guidelines to measurements of reproducible contact angles using a sessile-drop technique, Surf. Innovations 1 (4) (2013) 248–254.
[33] X.-L. Meng, L.-S. Wan, Z.-K. Xu, Insights into the static and advancing water contact angles on surfaces anisotropised with aligned fibers: Experiments and modeling, Colloids Surf., A 389 (1–3) (2011) 213–221.
[34] J.J.R.M. D"Angelo, P. Design, The Relationship of the MSCR Test to Rutting, 10 (sup1) (2009) 61-80.
[35] HildeSoenen, TimoBlomberg, TerhiPellinen, O.-V.J.R. Materials, P. Design, The multiple stress creep-recovery test: a detailed analysis of repeatability and reproducibility, 14(sup1) (2013) 2-11.
[36] Determining the Flexural Creep Stiffness of Asphalt Binder Using the Bending Beam Rheometer (BBR), AASHTO (T 313-09) (Standard Method of Test).
[37] S. Vassaux, V. Gaudefroy, L. Boulangé, A. Pévère, V. Mouillet, V. Barragan-Montero, Towards a better understanding of wetting regimes at the interface asphalt/aggregate during warm-mix process of asphalt mixtures, Constr Build Mater 133 (2017) 182–195.
[38] C. Peng, H. Zhang, Z. You, F. Xu, G. Jiang, S. Lv, R. Zhang, H. Yang, Preparation and anti-icing properties of a superhydrophobic silicone coating on asphalt mixture, Constr Build Mater 189 (2018) 227–235.